ISSN 2176-5480

22nd International Congress of Mechanical Engineering (COBEM 2013)
November 3-7, 2013, Ribeirão Preto, SP, Brazil

A COMPARATIVE ANALYSIS OF 3 AND 4-WHEEL AIR CYCLE MACHINES FOR AERONAUTICAL APPICATIONS

Cláudia Regina de Andrade
Edson Luiz Zaparoli
claudia@ita.br
zaparoli@ita.br
Instituto Tecnológico de Aeronáutica
Pça Marechal Eduardo Gomes, 50 - 12228-900 - São José dos Campos, SP, Brasil

Abstract. *Air cycle refrigeration is an attractive alternative that has been employed to provide aircraft cabin cooling. The primary function of the cabin air conditioning and pressurization system is to maintain an aircraft environment that will ensure safety and comfort of the passengers and crew during all fly operational conditions and provide adequate avionics cooling. The energy to drive these machines comes from the compressed air bleed from the compressor of the aircraft propulsion turbine. Usually, ACM (Air Cycle Machine) architecture includes mainly two compact air-to-air heat exchangers, a compressor and a expander with one or two expansion stages (called 3-whell or 4-whell configuration, respectively). At this context, this work focuses on a comparative thermodynamic study of 3 and 4 wheels air-conditioning aircraft air cycle machines. This comparison will be performed taking account some design features that affect the ACM performance as: aircraft flight Mach number, cabin altitude, heat exchanger effectiveness and compressed bleed air conditions. Results showed that the second level of expansion from 4-wheel air cycle machine increases its thermodynamic efficiency. As the amount of rejected heat in the secondary heat exchanger (SHX) is greater for the 4-wheel architecture, it is possible to have the same cooling effect than the 3-wheel machine but with a more compact SHX. Besides, the implemented computational tool to solving the air cycle refrigeration mathematical model allows a better understanding of the ACM performance.*

Keywords: *air conditioning, Air Cycle Machine (ACM), Environmental Control System (ECS), Coefficient of Performance (COP).*

1. INTRODUCTION

Aircraft Environmental Control Systems (ECS) must be able to isolate occupants from outside weather (Lombardo, 1999). These systems involve processes that either remove or add heat to provide both a comfortable environment to the aircraft passengers and operable conditions to the electrical equipment. This includes a supply of conditioned air for heating and cooling the cockpit and cabin spaces. Hence, design conditions for aircraft applications differ in several ways from other stationary air conditioning applications. Commercial transport aircraft operate in a physical environment that requires suitable ventilation, heating, cooling, humidity/contamination control, and pressurization in the occupied compartments, cargo space, and electronic avionic bays. Therefore, the air-conditioning packs must provide essentially dry, sterile, and dust free conditioned air to the airplane cabin at the proper temperature, flow rate, and pressure to satisfy pressurization and temperature control requirements, Hunt et al (1995). Also aircraft systems must be light, accessible for quick inspection and servicing, highly reliable, tolerant of a wide range of environmental conditions, able to withstand aircraft vibratory and maneuver loads, and able to accommodate failures occurring during flight, ASRHAE (2007).

Air refrigeration cycle is a tried and tested technology that has long been the basis of aircraft cabin cooling. The use of air as a refrigerant is based on the principle that when a gas expands isentropically from a given temperature, its final temperature at the new pressure is much lower. The resulting cold gas can then be used as a refrigerant, either directly in an open system, or indirectly by means of a heat exchanger in a closed system.

The present day gas turbine aircrafts have very high cooling loads because of their large occupancy, electronic equipment and high velocity with consequent heat generation due to skin friction. The main considerations involved in an aircraft application in order of importance are weight, space and operating power, since weight and space results in severe fuel penalties. Usually, compressed air extracted from one or more stages of the engine compressor expands through a turbine with the power extracted used to drive a fan (simple cycle), a compressor (bootstrap cycle), or both (simple/bootstrap cycle). The power extraction and expansion of the compressor air across the turbine results in a significant temperature decrease. This air provides cooling of the aircraft occupied compartments and avionics. Some of the bleed air from the engines can be bypassed around the air-conditioning pack if warm is need in the cabin, Garret (1991).

Air cycle machines are lighter and more compact than vapour refrigeration systems (Moir and Seabridge, 2001). Some additional advantages of an air cycle with regard to its application in aircraft refrigeration are pointed out byArora (1988) as: (i) high ventilation rate necessary for the pressurized aircraft cabin; (ii) high flow rate of compressed air for

ISSN 2176-5480

cabin pressurization; (iii) part of compression work can be attributed to cabin pressurization; (iv) one only equipment for cooling/heating; and ((v) allows cabin air-conditioning/pressurization integration.

Different characteristics of air-cycle refrigeration has been investigated by several researches. Conceição et al (2007) developed a thermodynamic model of an air-cycle machine under flight and ground operating conditions. Their results showed that the thermodynamic advantages of the 4-wheel in relation to the 3-wheel machine are maximized when considering critical cooling conditions for hot days.

Al-Garni et al (2009) developed a tool for extracting management information from field failures of aircraft cooling systems. Their techniques allow engineers to quickly identify failure trends, misbehaving systems, unusual behaviors, the effects of environmental conditions, maintenance practices, repair actions for ECS system maintenance.

Tu and Lin (2011) showed that the thermal dynamic responses of the air-cycle cooling pack is sensible to the temperature and the mass-flow-rate change of bleed air and ram air. Yoo et al (2011) developed an air-cycle machine modeling program, including a phase change heat exchanger, to estimate its effect in various aircraft flight conditions such as take-off, maneuver, cruise, and landing.

At this context, the present work focuses on the numerical simulation comparing 3-wheel and 4-wheel air cycle machines performance. These two configurations are simulated changing the following parameters: flight Mach number, cabin altitude, ACM secondary heat exchanger effectiveness, and pressure at bleed control valve exit. Results showed that the second level of expansion from 4-wheel air cycle machine increases the thermodynamic efficiency of the air refrigeration system.

2. FLIGHT SCENARIO AND AIR CYCLE MACHINES

Aircraft air conditioning/pressurization systems insufflate air into the cabin taking account that a significant internal stress is placed upon the fuselage´s skin, (Lombardo, 1993). All modern aircraft has a cabin pressure control system continuously monitors the airplane's ground and flight modes, altitude, climb, cruise, or descent modes as well as the airplane's holding patterns at various altitudes. It uses this information to allow air to escape continuously from the airplane by further opening or closing the cabin pressure outflow valve in the lower aft fuselage. The outflow valve is constantly being positioned to maintain cabin pressure as close to sea level as practical.

Cabin altitude and pressure changes are much smaller in magnitude on today's high altitude pressurized jets than they were during past flights. Although the percentage of oxygen in cabin air remains virtually unchanged (21 percent) at all normal flight altitudes compared to sea level, the partial pressure of oxygen decreases with increasing altitude. This is because with increasing altitude air is less densely packed, resulting in fewer molecules of oxygen available for each occupant breathing cycle (Hunt and Space, 1994).

A typical flight will cruise at 30,000 to 36,000 feet, maintaining a cabin altitude of 8,000 feet. This differential pressure results in a cabin wall structural effort, as depicted in Figure 1.

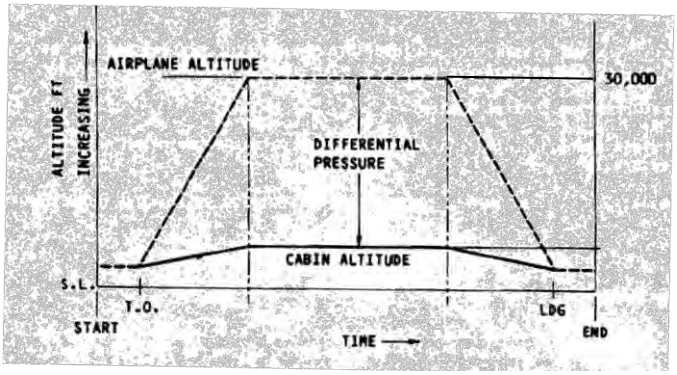

Figure 1 - A typical cabin altitude schedule.

An air-conditioning pack is an air cycle refrigeration system that uses the air passing through and into the airplane as the refrigerant fluid. This is accomplished by a combined turbine and compressor machine, valves for temperature and flow control, and heat exchangers using outside ram-air to dispense waste heat. The ACM must provide essentially dry, sterile, and dust free conditioned air to the airplane cabin at the proper temperature, flow rate, and pressure to satisfy pressurization and temperature control requirements (Hunt et al., 1995).

There are four usual configurations of ACM where compressed air extracted from the propulsion turbine compressor is cooled (by one or two heat exchangers) and expanded through a turbine. The power supplied by the ACM turbine may be used to drive:

- a fan (simple cycle, Figure 2a),
- a compressor (2-wheel bootstrap cycle, Figure 2b),

ISSN 2176-5480

- a compressor and a one-stage expansion turbine (3-wheel cycle, Figure 2c) or
- a compressor and two-stages expansion turbine (4-wheel cycle, Figure 2d).

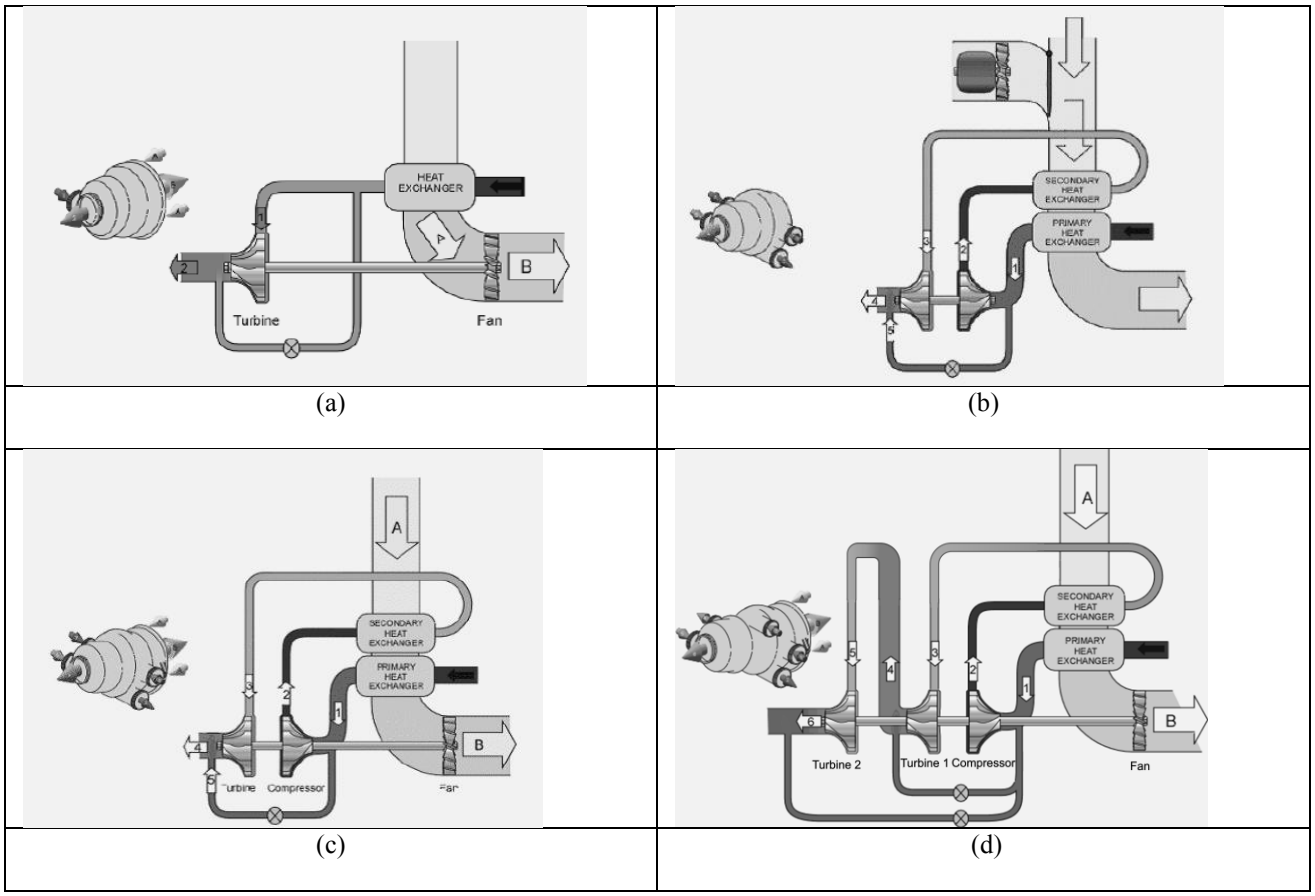

Figure 2 - Typical air cycle machines: (a) simple cycle; (b) 2-wheel bootstrap cycle; (c) 3-wheel cycle, and (d) 4-wheel cycle.

In the simple cycle, all the ACM turbine work is consumed by the exhaust fan while in the full bootstrap cycle (2-wheel machine) this work is used only to drive the ACM compressor. In the 3-wheel cycle, the turbine work drives both compressor and exhaust fan. The 4-wheel configuration has two turbines, a compressor and a fan in a common shaft.

3. THERMODYNAMIC MODELING

3.1 - 3-wheel ACM

Thermodynamic processes (1-7) for 3-wheel air cycle machine (ACM) are represented in the temperature x entropy diagram, Figure 3a. When the aircraft is flying, the initial compression of the ambient air is due to ram effect. The ram effect is shown by process 1-2. Point 1 represents the static temperature and pressure of external ambient air, while point 2i denotes the state after isentropic compression to pressure P2i and temperature T2i so that we have from the energy equation:

$$h_2 = h_1 + \frac{V_1^2}{2} \qquad \text{Eq. 1}$$

where:
h_1 = static air enthalpy.
V_1 = aircraft velocity.

Assuming air as a perfect gas with constant specific heat, from Eq. 1, the following result is obtained:

ISSN 2176-5480

$$T_2 = T_{2i} = T_1 + \frac{V_1^2}{2Cp} \qquad \text{Eq. 2}$$

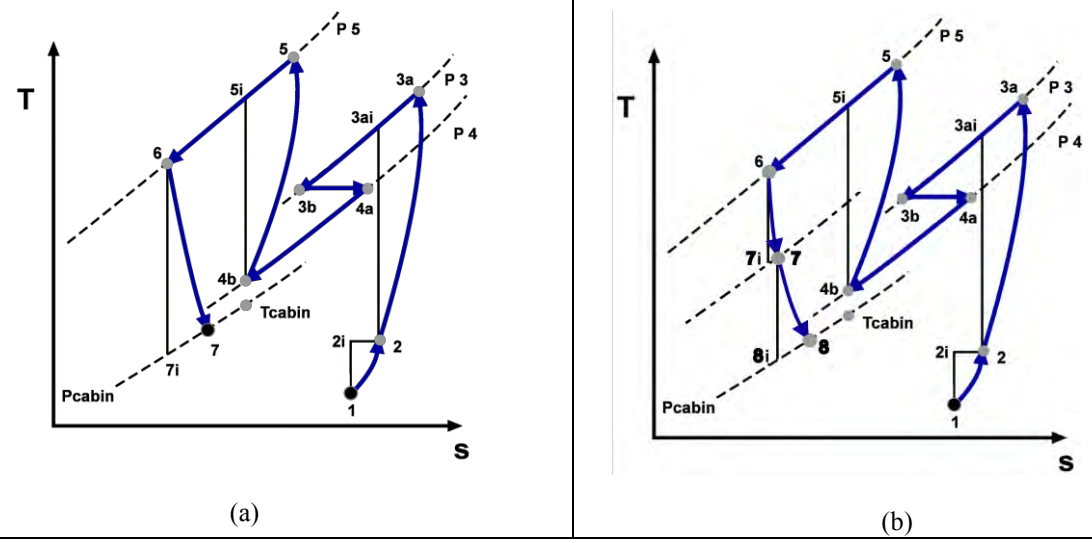

With:

1	ambient static conditions;
2	state after ram air compression;
3a	propulsion turbine compressor (primary compressor) exit;
3b	bleed pre-cooler (heat exchanger) exit;
4a	pressure at bleed control valve exit;
4b	ACM primary heat exchanger exit;
5	ACM compressor (secondary compressor) exit;
6	ACM secondary heat exchanger exit;
7	ACM primary turbine exit;
8	ACM secondary turbine exit;
i	isentropic process exit;
cabin	aircraft cabin conditions.

Figure 3 - Thermodynamic processes for (a) 3-wheel and (b) 4-wheel ACM machines.

The above relation can be modified such that the Mach number appears:

$$\frac{T_2}{T_1} = 1 + \frac{(k-1)M^2}{2} \qquad \text{Eq. 3}$$

where:
k = C_p/C_v = specific heat relation: constant pressure to constant volume;
M = Mach number of the aircraft flight = V_1/a;
a = sound velocity.

The stagnation pressure after isentropic compression P_{2i}, is given by the relation:

$$\frac{P_{2i}}{P_1} = \left(\frac{T_{2i}}{T_1}\right)^{\frac{k}{k-1}} \qquad \text{Eq. 4}$$

The irreversible ram compression, however, results in air reaching point 2 instead of point 2i, that is, at the same stagnation temperature but at a reduced stagnation pressure P_2 which is obtained from the knowledge of the ram efficiency (η_r) defined by:

ISSN 2176-5480

$$\eta_r = \frac{P_2 - P_1}{P_{2i} - P_1} = \frac{actual\ \ pressure\ recovery}{ideal\ \ pressure\ recovery} \quad \text{Eq. 5}$$

The ram work (W_r) which is obtained directly from the engine (drag penalty) is evaluated by:

$$W_r = \dot{m} Cp\,(T_2 - T_1) \quad \text{Eq. 6}$$

$\dot{m}$ = mass flow rate.

The rest of compression occurs at the propulsion turbine compressor, process 2-3a. For the ideal isentropic process 2-3_{ai} the temperature at the point 3i is calculated as:

$$\frac{T_{3ai}}{T_2} = \left(\frac{P_3}{P_2}\right)^{\frac{k-1}{k}} \quad \text{Eq. 7}$$

Where P_3 = compressor bleed port pressure.

The temperature at the point 3a (primary compressor bleed port) is determined with the value of its isentropic efficiency (η_{pc}), defined by:

$$\eta_{pc} = \frac{T_{3ai} - T_2}{T_{3a} - T_2} = \frac{ideal\ \ \ primary\ compressor\ \ work}{actual\ \ primary\ compressor\ \ work} \quad \text{Eq. 8}$$

The actual primary compressor work can be calculated by:

$$W_{pc} = \dot{m} Cp\,(T_{3a} - T_2) = \frac{\dot{m} Cp T_2}{\eta_{pc}} \left[\left(\frac{P_3}{P_2}\right)^{\frac{k-1}{k}} - 1 \right] \quad \text{Eq. 9}$$

The aircraft bleed system controls the temperature and pressure of the compressed air. The state of compressed air supplied to the air cycle machine is represented by point 4a in T x s diagram shown in Figure 3b. The temperature drop in the pneumatic system pre-cooler (3a-3b) doesn't represent a performance penalty but the pressure reduction through the pneumatic pressure control valve (3b-4a) causes a lost in the cooling effect.

In the process 4a-4b the working fluid (air) is cooled by the ACM primary heat exchanger. Pressure P4a is equal to P4b if the fluid friction process is neglected. The amount of heat rejected in the ACM primary heat exchanger (Q_{phx}) is:

$$Q_{phx} = \dot{m} Cp\,(T_{4a} - T_{4b}) \quad \text{Eq. 10}$$

Where T_{4b} is calculated taking account the primary heat exchanger effectiveness (ε_{phx}) given by:

$$\varepsilon_{phx} = \frac{T_{4a} - T_{4b}}{T_{4a} - T_2} \quad \text{Eq. 11}$$

assuming that the heat sink (ram air) temperature of the primary heat exchanger is equal to T_2.

The temperature after the cooling process 4a-4b must be higher than the stagnation temperature T_2 of the heat sink ram air. It implies that the working fluid cannot be cooled by the heat exchange to a temperature bellow T_2. Temperature at the point 5i, after the isentropic compression through the ACM secondary compressor, is calculated as:

ISSN 2176-5480

$$\frac{T_{5i}}{T_{4b}} = \left(\frac{P_5}{P_{4b}} \right)^{\frac{k-1}{k}} \quad \text{Eq. 12}$$

Given the value of the secondary compressor isentropic efficiency, the temperature at the point 5 can be determined as:

$$\eta_{sc} = \frac{T_{5i} - T_{4b}}{T_5 - T_{4b}} = \frac{ideal \;\; sec ondary \; compressor \; work}{actual \; sec ondary \; compressor \; work} \quad \text{Eq. 13}$$

The actual secondary compressor work can be calculated by:

$$W_{sc} = \dot{m} Cp \, (T_5 - T_{4b}) = \frac{\dot{m} Cp T_{4b}}{\eta_{sc}} \left[\left(\frac{P_5}{P_4} \right)^{\frac{k-1}{k}} - 1 \right] \quad \text{Eq. 14}$$

In the process 5-6 the working fluid (air) is cooled by the ACM secondary heat exchanger. If the pressure loss is neglected, pressure P_5 is equal to P_6. The amount of heat rejected in the ACM secondary heat exchanger (Q_{shx}) is:

$$Q_{shx} = \dot{m} Cp \, (T_5 - T_6) \quad \text{Eq. 15}$$

Where T_6 is calculated taking account the secondary heat exchanger effectiveness (ε_{shx}) given by:

$$\varepsilon_{shx} = \frac{T_5 - T_6}{T_5 - T_2} \quad \text{Eq. 16}$$

assuming that the minimum attainable temperature for the working fluid is the ram air temperature.

The largest temperature drop occurs when the air expands in the turbine (expander) of the air cycle machine. In the isentropic process the state at the end of expansion process is represented by point 7i in T x s diagram (Figure 3). For the actual conditions, the pressure P7i = P7 is slightly above the pressure of aircraft pressurized cabin (Pcabin) that is higher than the external ambient pressure. At the present work, it is assumed that P7 = Pcabin , neglecting the pressure drop in the air distribution ducts.

Pressure P_5 (= P_6) is determined solving the implicit equation obtained from the ACM work balancing: the ACM turbine work is equal to the sum of the secondary compressor work and the exhaust fan work. Temperature T_{7i} can be calculated by the isentropic relation:

$$\frac{T_{7i}}{T_6} = \left(\frac{P_7}{P_6} \right)^{\frac{k-1}{k}} \quad \text{Eq. 17}$$

Due to expansion irreversibility, temperature T_7 is greater than T_{7i} reducing the expander temperature drop. The temperature T_7 at the end of the actual expansion process can be calculated knowing the turbine isentropic efficiency (η_{tl}):

$$\eta_t = \frac{T_6 - T_7}{T_6 - T_{7i}} = \frac{actual \;\; turbine \, work}{isentropic \;\; turbine \, work} \quad \text{Eq. 18}$$

ISSN 2176-5480

The ACM turbine useful work is calculated as:

$$W_{t1} = \dot{m}Cp\,(T_6 - T_7) = \dot{m}CpT_6 \left[1 - \left(\frac{P_7}{P_6}\right)^{\frac{k-1}{k}}\right]\eta_{t1} \quad \text{Eq. 19}$$

The 3-wheel ACM work balance is given by:

$$W_{sc} = \alpha\,(W_{t1}) \quad \text{Eq. 20}$$

Where α indicates the percentage of the ACM turbine work absorbed by the secondary compressor. The available work to drive the heat exchanger exhaust fan is equal to $(1 - \alpha)\, W_{t1}$.

Inserting Eq. 14 and Eq. 19 in Eq. 20, the implicit equation that provides the P_5 value is obtained:

$$\frac{\dot{m}CpT_{4b}}{\eta_{sc}}\left[\left(\frac{P_5}{P_4}\right)^{\frac{k-1}{k}} - 1\right] - \alpha\left\{\dot{m}CpT_6\left[1 - \left(\frac{P_7}{P_5}\right)^{\frac{k-1}{k}}\right]\eta_{t1}\right\} = 0 \quad \text{Eq. 21}$$

When $\alpha = 0$, the exhaust fan uses all the ACM turbine work (simple cycle) and for $\alpha = 1$, the secondary compressor absorbs the whole turbine work (bootstrap cycle).

The air circulated through the air cycle machine is insufflated in the aircraft cabin with temperature T_7, that should be lower than the inside air temperature T_{cabin}. The cooling effect of the air cycle machine (Q_c) is calculated by:

$$Q_c = \dot{m}Cp\,(T_{cabin} - T_7) \quad \text{Eq. 22}$$

A portion of the primary compressor work must be attributed to the cabin pressurization system This work is used to increase the external air pressure to an adequate value that satisfies the human breathing requirements attaining a desirable occupants comfort level (usually a pressure value in the 8,000 ft level in the standard atmosphere, Figure 1. The pressurization work (W_p) can be calculated by:

$$W_p = \frac{\dot{m}CpT_2}{\eta_{pc}}\left[\left(\frac{P_7}{P_2}\right)^{\frac{k-1}{k}} - 1\right] + W_r \quad \text{Eq. 23}$$

The coefficient of performance (*COP*) for the 3-wheel air-cycle, including the pressurization work, can be evaluated as:

$$COP = \frac{Q_c}{W_r + W_{pc}} \quad \text{Eq. 24}$$

Excluding the pressurization work (Eq. 23), coefficient of performance (COP_p) for the 3-wheel air-cycle is calculated by:

$$COP_P = \frac{Q_c}{W_r + W_{pc} - W_p} \quad \text{Eq. 25}$$

ISSN 2176-5480

3.1 - 4-wheel ACM

Until air-state 7 (Eq. 16), 3 and 4-wheel ACMs perform the same processes, see Figure 3b. However, it should be observed that the state of the air insufflated into the cabin is determined by T7 and P7 = Pcabin, for 3-wheel machine, while T7 and P7 determine the air-state at the primary turbine exit for 4-wheel ACM, Figure 4b. Air state at the secondary turbine exit is now represented by T8 and P8 = Pcabin. Temperature T8i can be calculated by the isentropic relation:

$$\frac{T_{8i}}{T_7} = \left(\frac{P_8}{P_7}\right)^{\frac{k-1}{k}} \qquad \text{Eq. 26}$$

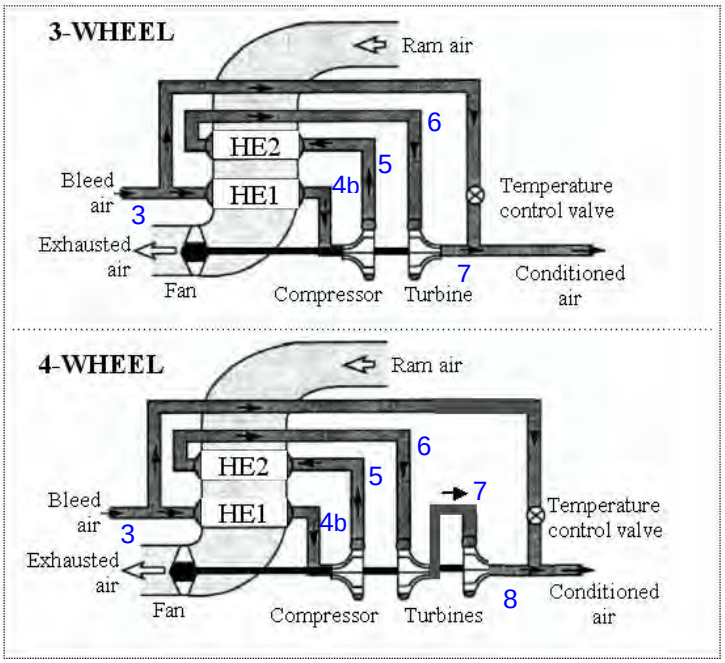

(a)

(b)

Figure 4 - Schematic representation of 3-wheel (a) and 4-wheel (b) air-cycle machines.

Due to expansion irreversibility, temperature T_8 is greater than T_{8i} reducing the secondary expander temperature drop. The temperature T_8 at the end of the actual second stage process can be calculated knowing the secondary turbine isentropic efficiency (η_{t2}):

$$\eta_{t2} = \frac{T_7 - T_8}{T_7 - T_{8i}} = \frac{actual\ \ secondary\ \ turbine\ work}{isentropic\ secondary\ turbine\ work} \qquad \text{Eq. 27}$$

The ACM secondary turbine useful work is calculated as:

$$W_{t2} = \dot{m}Cp\,(T_7 - T_8) = \dot{m}CpT_7\left[1 - \left(\frac{P_8}{P_7}\right)^{\frac{k-1}{k}}\right]\eta_{t2} \qquad \text{Eq. 28}$$

The 4-wheel ACM work balance is given by:

$$W_{sc} = \alpha\left(W_{t1} + W_{t2}\right) \qquad \text{Eq. 29}$$

ISSN 2176-5480

Where α indicates the percentage of the ACM turbine work absorbed by the secondary compressor. The available work to drive the heat exchanger exhaust fan is equal to (1 - α) W_{sc}.

In the 4-wheel machine, P_7 can vary in the range P_6 to $P_8 = P_{cabin}$. To represent the sharing of available work between the two turbines which drives the secondary compressor, a beta parameter (β) can be defined as:

$$W_{t1} = \beta\,(W_{sc}) \qquad \text{Eq. 30}$$

and

$$W_{t2} = (1-\beta)\,W_{sc} \qquad \text{Eq. 31}$$

When $P_7 = P_6$, β is equal to zero ($W_{t1} = 0$) and β is equal to unitary ($W_{t2} = 0$) if $P_7 = P_8 = P_{cabin}$.

4. RESULTS AND DISCUSSION

All herein results were obtained with constant ambient static conditions (point 1, in Figure 3). Other constant parameters are also listed in Table 1, as follow: ACM turbines and compressors efficiencies, ram air compression efficiency, pressure and temperature values at primary compressor exit (point 3a, in Figure 3) and heat exchangers effectiveness. Besides, all simulations were performed with $\alpha = 1$ (see Eq. 20 and Eq. 29).

Table 1 -Numerical values maintained as constant parameters in the simulations.

$T_1 = -57^oC$	$P_1 = 20\ kPa$	$P_3 = 250\ kPa$	$T_{3b} = T_{4a} = 200^oC$
$\eta_{t1} = \eta_{t2} = 0.77$	$\eta_r = 0.84$	$\eta_{pc} = \eta_{sc} = 0.82$	$\varepsilon_{phx} = 0.80$

The influence of the sharing of available work between the two turbines (β parameter in Eq. 30 and Eq. 31) on air cycle machine performance is shown in Figure 5. Note that, when $\beta = 0$ or $\beta = 1$, the 4-wheel machine behavior reduces to the 3-wheel one.

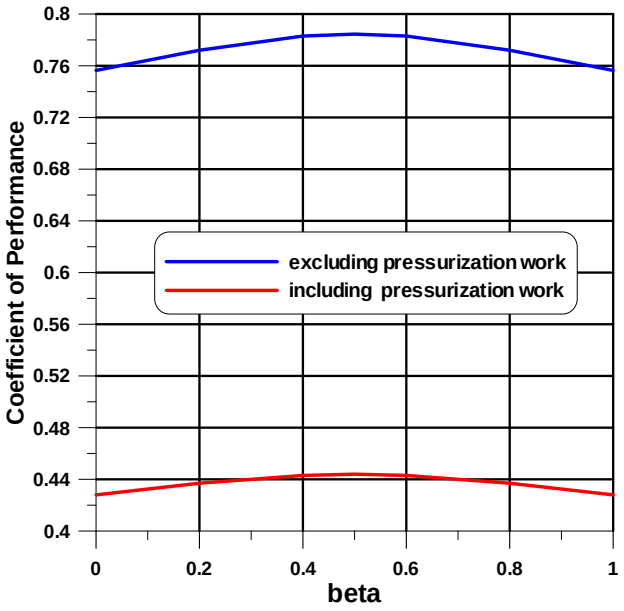

Figure 5 - Coefficient of Performance (COP and COP_p) as a function of the beta parameter (Ma = 0.47, Cabin altitude = 8,000 ft, P_4 = 200 kPa and $\varepsilon_{shx} = 0.80$)

The maximum coefficient of performance values are obtained for $\beta = 0.5$ that corresponds to $W_{t1} = W_{t2}$. This effect was observed for both cases: including and excluding pressurization work, denoted by Eq. 24 and Eq. 25, respectively. When the pressurization work is not computed, the air-cycle machine performance takes account only the

ISSN 2176-5480

required work to refrigerate the cabin air. This is the needed work, for example, if an independent vapour cycle would be used as the refrigerating aircraft system instead of the ACM option.

Figure 6 shows the available work associated with each turbine stage for the 4-wheel air-cycle machine (using the same efficiency values). As expected, these values are complementary as the β value varies, i.e., work totally generated by the primary turbine ($\beta = 1$) and by the secondary one ($\beta = 0$). Observe that the expansion work is maximum and equally split between the two turbines for $\beta = 0.5$.

Another important feature of the air-cycle machine is the amount of rejected heat in the secondary heat exchanger which is related with its required size and weight. Figure 7 presents that the amount of rejected heat has its inferior limit when $\beta = 0$ *or* $\beta = 1$ (3-wheel machine cases) and increases as the 4-wheel configuration takes place. The maximum is reached for $\beta = 0.5$, when the two turbines work is been shared. These results indicate that 4-wheel ACM provides a greater temperature drop across the secondary heat exchanger when compared with 3-wheel architecture.

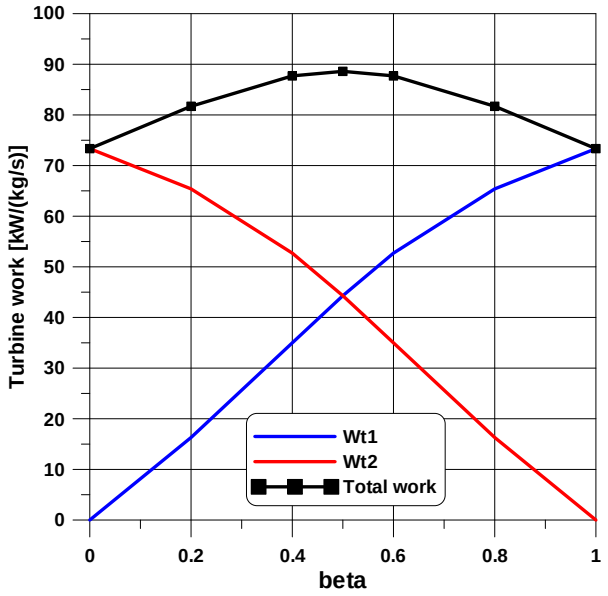

Figure 6 - Turbine work as a function of the beta parameter (P_{cabin} = 8,000 ft and $\eta_{t1} = \eta_{t2} = 0.77$).

Figure 7 also shows the ACM cooling effect as a function of the β parameter (total turbine work sharing). Once the secondary exchanger exit temperature is lower in the 4-wheel machine (state 6, in Figure 4), the refrigerating effect is also more intense in comparison with 3-wheel configuration (when $\beta = 0$ or $\beta = 1$). This advantage in the cooling efficiency is greater for $\beta = 0.5$, as expected.

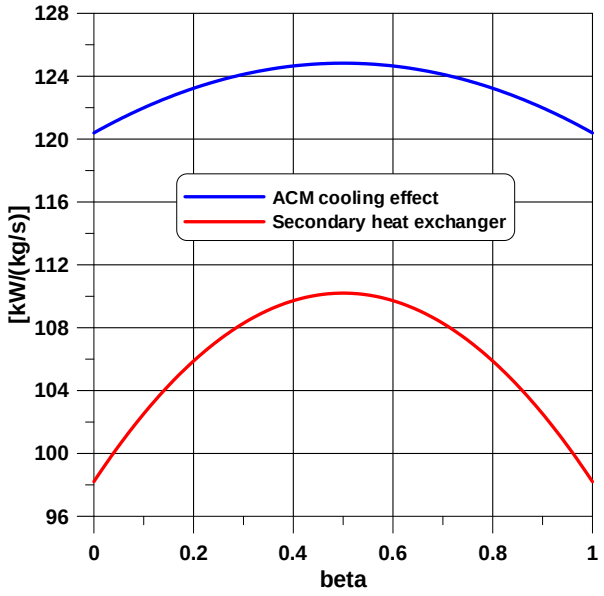

Figure 7 - Amount of rejected heat in the secondary HX and ACM cooling effect as a function of the beta parameter (P_{cabin} = 8,000 ft and $\eta_{t1} = \eta_{t2} = 0.77$).

ISSN 2176-5480

As the 4-wheel ACM with $\beta = 0.5$ possesses the best results, all remaining studies has been performed using this configuration. Figure 8 compares 3-wheel and 4-wheel performance as a function of the flight Mach number. It is verified that COP value decreases as the Ma number elevates for both ACM architectures. This is because if T_2 temperature increases the ram work (Eq. 6) is also higher, reducing the COP value (see Eq. 24).

Figure 8 also presents the effect of cabin altitude variation (6,000 and 8,000 ft) on the ACM performance. Note that when the cabin altitude is lower (higher cabin internal pressure) the COP value decreases. This fact can be explained remembering that the required work to cabin pressurization (Eq. 23) increases from 8,000 to 6,000 ft, resulting in a COP reduction (see Eq. 24). However, the 4-wheel machine exhibits a better performance when compared with 3-wheel machine: the COP value at 6,000 ft (4-wheel case) is even higher than the COP at 8,000 ft when the 3-wheel configuration is tested. Therefore, the best ACM performance is reached at low Ma number and 8,000 ft, and employing the 4-wheel architecture.

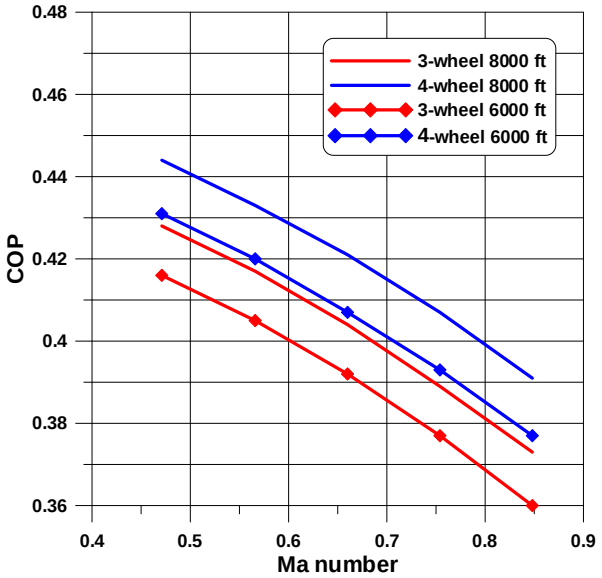

Figure 8 - Coefficient of Performance (COP) as a function of the Ma number: 3-wheel x 4-wheel machines ($\beta = 0.5$).

Figure 9 illustrates the ACM performance as a function of the secondary heat exchanger effectiveness at Ma = 0.47. This parameter is important because the amount of heat rejected in this component affect the inlet temperature (state 6, in Figure 4) in the ACM turbine. Hence, after the state 6 (secondary heat exchanger exit), the air will suffer only one-stage expansion (3-wheel machine, Figure 4a) or two-stages expansion (4-wheel machine, Figure 4b).

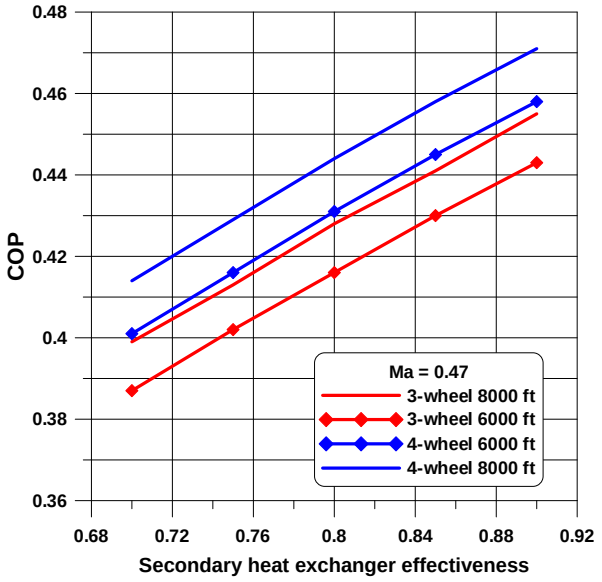

Figure 9 - Coefficient of Performance (COP) as a function of the secondary heat exchanger effectiveness (ε_{shx}): 3-wheel x 4-wheel machines ($\beta = 0.5$).

ISSN 2176-5480

As the secondary heat exchanger effectiveness increases the COP value also elevates for both 3-wheel and 4-wheel cases. Again, lower cabin altitude level implies in a COP reduction. This will be a trade-off design solution, because the cabin altitude decrease represents a more passenger comfortable condition (closest the sea level value).

The 3-wheel and 4-wheel air-cycle machines performance as a function of the compressed bleed air is shown in Figure 10 at Ma = 0.47. As the pressure at bleed control valve exit increases (state 4a in Figure 3).), it is observed an improvement in COP value for both 3-wheel and 4-wheel machines, although 4-wheel ACM presents higher performance. Note that at cabin altitude of 6,000 ft, the COP is higher than the 3-wheel machine at 8,000 ft.

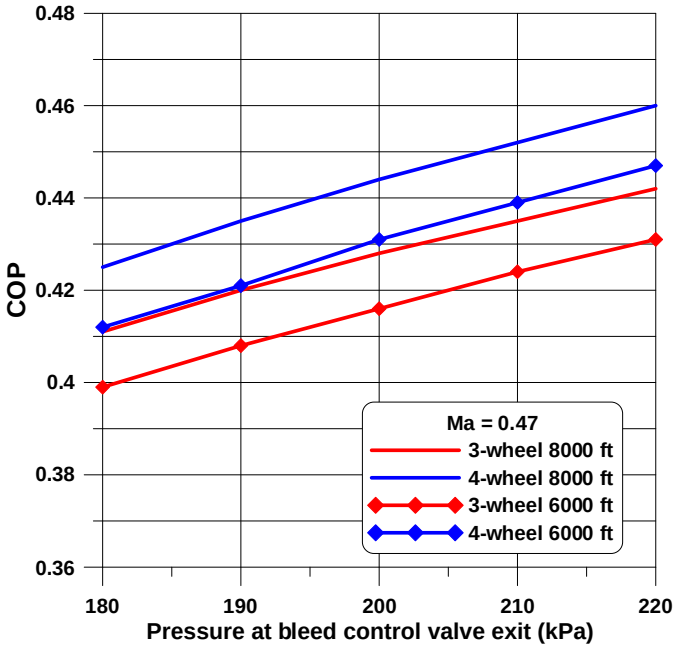

Figure 10 - Coefficient of Performance (COP) as a function of the pressure at bleed control valve exit: 3-wheel x 4-wheel machines ($\beta = 0.5$).

Table 2 - Temperature drop at different bleed air pressure levels

P_{4a} (kPa)	180	190	200	210	220
$\Delta T = T_{4a} - T_8$ (K)	295	298	300.3	302.6	305

The better COP values reached by 4-wheel machine can be also understood by observing the temperature drop listed in Table 2, when the pressure at bleed control valve exit varies. The temperature drop is more intense when P_{4a} = 220 kPa, resulting in a higher refrigerating effect (cabin insufflated air).

5. CONCLUDING REMARKS

Results obtained in this work showed that 4-wheel machine provides higher air-cycle COP values when compared with the 3-wheel configuration. The maximum performance is attained when the available turbine work is equally shared ($\beta = 0.5$ in Figure 6). Moreover, the rejected heat by the secondary heat exchanger (SHX) was also higher when two-stages expansion was employed. This superior behavior shown by 4-wheel architecture allows obtaining the same temperature drop than 3-wheel ACMs with more compact SHXs. This last feature is primordial for aeronautical application where size and weight restrictions are extremely significant.

6. REFERENCES

Al-Garni, A. Z., Tozan, M. and Abdelrahman, W. G, 2009, "Graphical Techniques for Managing Field Failures of Aircraft Systems and Components", Journal of Aircraft, 46(2), 608-616 pp.

Arora, C. P., 1988, "*Refrigeration and Air Conditioning*", Tata McGraw-Hill Publishing Company Limited, New Delhi, India, 726 p.

ISSN 2176-5480

ASHRAE Handbook, 2007, “HVAC Applications”, American Society of Heating, Refrigerating and Air-Conditioning Engineers, Inc., Atlanta, GA.

Conceição, S.T., Zaparoli, E.L. and Turcio, W.H.L., 2007, "Thermodynamic Study of Aircraft Air Conditioning Air Cycle Machine: 3-wheel x 4-wheel", *Proceedings of SAE Brazilian Congress*, Society of Automotive Engineers.

Garrett, A. D.,1991, “*Aircraft Systems & Components*”, Jeppesen Sanderson Inc., Englewwod, Colorado, USA.

Hunt, E.H. and Space, D.R., 1994, The Airplane Cabin Environment, *International In-flight Service Management Organization Conference*, Montreal, Canada.

Lombardo, D., 1993, “*Advanced Aircraft Systems*”, McGraw-Hill Publishing Company Limited, New York, USA.

Lombardo, D., 1999, “*Aircraft Systems*”, McGraw-Hill Publishing Company Limited, New York, USA.

Moir, I., Seabridge, A., 2001, “*Aircraft Systems: Mechanical, Electrical, and Avionics, Subsystems Integration*”, AIAA Education Series, Professional Engineering Publishing.

Tu, Y. and Lin, G.P. Dynamic Simulation of Aircraft Environmental Control System Based on Flowmaster, Journal of Aircraft, Vol. 48, No. 6, November–December 2011

Yoo, Y., Lee, H., Min, S. Hwang, K. and Lim, J., 2011, "A Study on a Modeling and Simulation Program of an Environmental Control System with a Phase Change Heat Exchanger", *AIAA Modeling and Simulation Technologies Conference,* Portland, Orego, USA.

7. RESPONSIBILITY NOTICE

The authors are the only responsible for the printed material included in this paper.